STATISTICS IN TRANSITION new series, March 2025
Vol. 26, No. 1, pp. 93–115, https://doi.org/10.59139/stattrans-2025-006
Received – 22.02.2024; accepted – 13.12.2024

Type I heavy-tailed family of generalized Burr III distributions: properties, actuarial measures, regression and applications

Wilbert Nkomo[1], Broderick Oluyede[2], Fastel Chipepa[3]

Abstract

This study introduces a new family of distributions (FoD) called type I heavy-tailed odd Burr III-G (TI-HT-OBIII-G) distribution. Several statistical properties of the family are derived along with actuarial risk measures. The maximum likelihood estimation (MLE) approach is adopted in the parameter estimation process. The estimates are evaluated centered on mean square errors and average bias via the Monte Carlo simulation framework. A regression model is formulated and the residual analysis is investigated. Members of the new FoD are applied to heavy-tailed data sets and compared to some well-known competing heavy-tailed distributions. The practicality, flexibility and importance of the new distribution in modeling is empirically proven using three data sets.

Key words: type I heavy-tailed-G, odd Burr III-G, parameter estimation, regression, actuarial measures.
Mathematics Subject Classification: 62E99, 60E05.

1. Introduction

Heavy-tailed distributions have high variances due to outliers with very high values. Modeling data with high variances using standard distributions has deficiencies since they lack flexibility in providing the good fit to heavy-tailed data sets. In a similar vein to rare occurrences such as earthquakes and cyclones, financial risks, such as insurance losses, often exhibit right-skewed data with heavy tails. This characteristic poses challenges for modeling such data using conventional methods.

[1] Department of Mathematics and Statistical Sciences, Botswana International University of Science and Technology, Botswana & Department of Applied Statistics, Manicaland State University of Applied Sciences, Zimbabwe. E-mail: nw22100009@studentmail.biust.ac.bw. ORCID: https://orcid.org/0009-0006-0277-3981.

[2] Department of Mathematics and Statistical Sciences, Botswana International University of Science and Technology, Botswana. E-mail: oluyedeo@biust.ac.bw. ORCID: https://orcid.org/0000-0002-9945-2255.

[3] Department of Mathematics and Statistical Sciences, Botswana International University of Science and Technology, Botswana. E-mail: chipepaf@biust.ac.b. ORCID: https://orcid.org/0000-0001-6854-8740.

Several authors have proposed generalized distributions to curb this inadequacy, for instance, Zhao et al. (2020) in their research proposed the type I heavy-tailed Weibull (TI-HT-W) distribution using the transformed-transformer (T-X) approach. They evaluated its suitability for analyzing the prevention of HIV progression with two antiretroviral drugs and compared it to the Weibull distribution. The findings demonstrated that the TI-HT-W distribution outperformed the Weibull distribution. The study aimed to enhance understanding of treatment strategies for HIV by providing insights into the effectiveness of different approaches contributing to advancements in HIV prevention and management. In their study, Dey et al. (2019) introduced a statistical distribution called the alpha power transformed inverse Lindley (APTIL) distribution. This distribution incorporates the inverse Lindley distribution and utilizes the alpha power transformation (APT), resulting in a versatile model with both scale and shape parameters. They found that the density function exhibited a single peak, indicating unimodality, and the hazard rate function (hrf) displayed a bathtub-shaped pattern, hence the distribution was found effective in analyzing lifetime data. Descheemaeker et al. (2021) studied complex ecological communities using stochastic Lotka-Volterra models with heavy-tailed abundance distributions. Their research focused on explaining how numerous species coexist within these communities and why rare species tend to dominate.

In situations where events exhibit very high deviations from the mean, surpassing what is expected based on the available baseline distributions, the application of heavy-tailed distributions becomes necessary. Heavy-tailed distributions are utilized to handle exceptional or uncommon events that defy explanation by conventional distributions. The literature presents diverse heavy-tailed distributions, offering mathematical models tailored to capture the distinctive characteristics of these events and provide more accurate probability estimates. Some recent advancements in the field of heavy-tailed distributions encompass various contributions including the heavy-tailed exponential by Affify et al. (2020), type II half logistical odd Fréchet by Alyami et al. (2022), alpha power Topp-Leone Weibull by Benkhelifa (2022) and heavy-tailed log-logistic by Teamah et al. (2021), among others. The motivations behind the development of this heavy-tailed distribution include:

(i) extending existing distributions using the TI-HT and the OBIII-G FoD.
(ii) expanding the parental distribution's adaptability in terms of density and hazard rate forms.
(iii) controlling the magnitude or influence of the tails in a parental distribution.
(iv) modeling and representing diverse data sets across multiple domains.

The paper follows the subsequent organization. We develop and present the new TI-HT-OBIII-G distribution including its sub-families and special cases in Section 2. Several statistical properties including moments, Rényi entropy and order statistics are

presented. Section 3 presents parameter estimation. Section 4 discusses risk measures and their numerical simulations. Section 5 discusses simulations and findings. The regression model is formulated in Section 6 while Sections 7 and 8 cover applications and conclusions, respectively.

2. The generalized distribution

The type I heavy-tailed odd Burr III-G (TI-HT-OBIII-G) family is developed in this section.

Zhao et al. (2020) proposed the type I heavy-tailed (TI-HT-G) FoD. The cumulative distribution function (cdf) of the TI-HT FoD is

$$F_{TI-HT-G}(x;\theta,\Omega) = 1 - \left(\frac{1-G(x;\Omega)}{1-(1-\theta)G(x;,\Omega)}\right)^{\theta} \tag{1}$$

and the probability density function (pdf) is

$$f_{TI-HT-G}(x;\theta,\Omega) = \frac{\theta^2 g(x;\Omega)\{1-G(x;\Omega)\}^{\theta-1}}{\{1-(1-\theta)G(x;\Omega)\}^{\theta+1}}, \tag{2}$$

for θ, $x > 0$, where Ω denotes the parameter vector from the baseline distribution $G(.)$.

Alizadeh et al. (2017) presented the odd Burr III-G (OBIII-G) FoD. The OBIII-G cdf is

$$F_{OBIII-G}(x;\, c,\, k,\, \Psi) = [1 + B_G(x;\, c,\, \Psi)]^{-k} \tag{3}$$

and the pdf is

$$f_{OBIII-G}(x;\theta,\Omega) = ckg(x;\Psi)\frac{[1-G(x;\Psi)]^{c-1}}{[G(x;\Omega)]^{c+1}}[1 + B_G\,(x;\; c,\Psi)]^{-k-1}, \tag{4}$$

for c, k, $x > 0$, and parameter vector Ψ, where $B_G\,(x;\; c,\Psi) = \left(\frac{1-G(x;\Psi)}{G(x;\Psi)}\right)^{c}$.

Replacing the baseline cdf in Equation (1) with the OBIII-G FoD yields the new FoD called TI-HT-OBIII-G with cdf

$$F(x;\; c,k,\theta,\Psi) = 1 - \left(\frac{1-[1 + B_G\,(x;\, c,\Psi)]^{-k}}{1-(1-\theta)[1 + B_G\,(x;\, c,\Psi)]^{-k}}\right)^{\theta} \tag{5}$$

and pdf

$$f(x;c,k,\theta,\Psi) = \frac{\theta^2 ckg(x;\Psi)\left[1+\left(\frac{1-G(x;\Psi)}{G(x;\Psi)}\right)^{c}\right]^{-k-1}(1-G(x;\Psi))^{c-1}}{(G(x;\Psi))^{c+1}}\left\{1-\left[1+\left(\frac{1-G(x;\Psi)}{G(x;\Psi)}\right)^{c}\right]^{-k}\right\}^{\theta-1}$$

$$\times\left\{1-(1-\theta)\left[1+\left(\frac{1-G(x;\Psi)}{G(x;\Psi)}\right)^{c}\right]^{-k}\right\}^{-(\theta+1)} \tag{6}$$

for $c, k, \theta > 0$ and baseline parameter vector Ψ. The model contains many sub-families by letting some of the parameters equal to unit.

2.1. Quantile function

The quantile function of the TI-HT-OBIII-G FoD is

$$Q_{X(u)} = G^{-1}\left[\left(1+\left[\left(\frac{1-(1-u)^{\frac{1}{\theta}}}{1-(1-u)^{\frac{1}{\theta}}[1-\theta]}\right)^{\frac{-1}{k}}-1\right]^{\frac{1}{c}}\right)\right]^{-1} \tag{7}$$

for $0 \le u \le 1$. To determine the quantile values of the TI-HT-OBIII-G FoD, the process involves solving Equation (7) and providing the baseline distribution G(.). The quantile function relies on the baseline cdf G(.), and the quantile values can be obtained by employing numerical methods in R software to solve the nonlinear equation. For more detailed derivations, please refer to the web **appendix**.

2.2. Linear representation

This subsection seeks to expand the density of the TI-HT-OBIII-G FoD. The density of the TI-HT-OBIII-G FoD can be represented in the form $f(x;\ c,k,\theta,\Psi) = \sum_{w=0}^{\infty}\eta_{w+1}g_{w+1}\ (x;\ \Psi)$ (8)

where $g_{w+1}(x; \Psi) = (w + 1)\, g\,(x; \Psi)\, G^{w}\,(x; \Psi)$ defines the exponentiated-G (Expon-G) distribution, $(w + 1)$ is the power parameter and

$$\eta_{w+1} = \sum_{r,s,t,v=0}^{\infty}\ (-1)^{r+s+v+w}(1-\theta)^{r}\mathrm{ck}\,\theta^{2}\binom{-(\theta+1)}{r}\binom{\theta-1}{s}\binom{\frac{1}{w+1}}{} \times\binom{-[1+k(s+r+1)]}{t}\binom{-[1+c(t+1)]}{v}\binom{v+c(t+1)-1)}{w}. \tag{9}$$

As a result, the pdf of the TI-HT-OBIII-G FoD can be presented as an unbounded linear mixture of the exponentiated-G (Expon-G) densities. This representation allows for the direct deduction of structural properties associated with the TI-HT-OBIII-G FoD. The web **appendix** contains detailed derivations of the density expansion and explores structural properties, including moments, order statistics, and Rényi entropy.

2.3. Special cases

This subsection presents some special cases of TI-HT-OBIII-G FoD by specifying $G\,(x; \Psi)$ and $g\,(x; \Psi)$ in Equation (5) and Equation (6).

2.3.1. Type I heavy-tailed odd Burr III-Weibull distribution

Considering the Weibull distribution with cdf $G\,(x; \lambda) = 1-\exp(-x^{\lambda})$ and pdf

$g(x;\lambda) = \lambda x^{\lambda-1}\exp(-x^{\lambda})$, for $\lambda, x > 0$, as the baseline distribution, we have the Type I heavy-tailed odd Burr III-Weibull (TI-HT-OBIII-W) distribution defined by the cdf

$$F(x;\theta,\lambda,c,k) = 1 - \left(\frac{1-[1+B_1(x;c,\lambda)]^{-k}}{1-(1-\theta)[1+B_1(x;c,\lambda)]^{-k}}\right)^{\theta},$$

and pdf

$$f(x;\theta,\lambda,c,k) = \frac{\theta^2 ck\lambda x^{\lambda-1}[1+B_1(x;c,\lambda)]^{-k-1}\exp\left(-x^{\lambda}\right)^{c}}{\left(1-\exp(-x^{\lambda})\right)^{c+1}(1-(1-\theta)[1+B_1(x;c,\lambda)]^{-k})^{(\theta+1)}} \times\{1-[1+B_1(x;c,\lambda)]^{-k}\}^{\theta-1}$$

for $\theta,\lambda,c,k > 0$, where $B_1(x;c,\lambda) = \left(\frac{\exp(-x^{\lambda})}{1-\exp(-x^{\lambda})}\right)^{c}$.

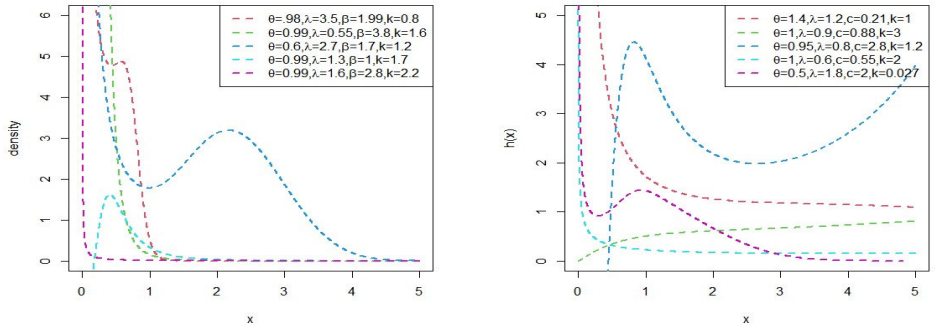

Figure 1: TI-HT-OBIII-W distribution's density and hrf plots

Figure 1 illustrates several density plots and hrf plots for the TI-HT-OBIII-W distribution. The TI-HT-OBIII-W density is capable of handling data that is right-skewed as well as reversed-J shaped. The hrf exhibits a variety of geometric configurations, such as decreasing, increasing, and bathtub-shaped followed by inverted bathtub-shaped patterns, as well as inverted bathtub-shaped followed by bathtub-shaped patterns.

2.3.2. Type I heavy-tailed odd Burr III-Kumaraswamy distribution

The type I heavy-tailed odd Burr III-Kumaraswamy (TI-HT-OBIII-Kum) distribution can be considered by utilizing the Kumaraswamy distribution as the baseline. The cdf and pdf of Kumaraswamy distribution are characterized by $G(x; a, b) = 1 - (1 - x^{a})^{b}$ and $g(x; a, b) = abx^{a-1}(1 - x^{a})^{b-1}$ respectively, for $a, b, x > 0$. The cdf of TI-HT-OBIII-Kum distribution is

$$F(x;b,a,\theta,c,k) = 1 - \left(\frac{1-[1+B_2(x;b,a,c)]^{-k}}{1-(1-\theta)[1+B_2(x;b,a,c)]^{-k}}\right)^{\theta}$$

and the pdf is

$$f(x;b,a,\theta,c,k) = \frac{\theta^2 abck(x)^{a-1}[1+B_2(x;b,a,c)]^{-k-1}[(1-x^a)^b]^{c-1}}{(1-(1-x^a)^b)^{c+1}(1-(1-\theta)[1+B_2(x;b,a,c)]^{-k})^{(\theta+1)}} \times \{1-[1+B_2(x;b,a,c)]^{-k}\}^{\theta-1},$$

for $a,b,c,k,\theta,x>0$, where $B_2(x;b,a,c) = \left(\frac{(1-x^a)^b}{1-(1-x^a)^b}\right)^c$.

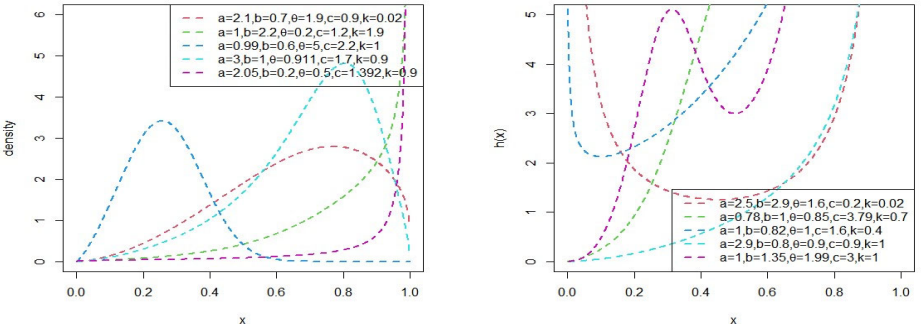

Figure 2: Density and hrf plots for the TI-HT OBIII-Kum distribution.

Figure 2 reveals the density and hrf plots corresponding to the TI-HT-OBIII-Kum distribution. The pdf of the TI-HT-OBIII-Kum distribution is suitable for analyzing data that display positive skewness, negative skewness, and J-shaped pattern. The hrf exhibits both monotonically increasing and nonmonotonically increasing patterns.

2.3.3. Type I-heavy tailed odd Burr III-Pareto distribution

The cdf and pdf of the Pareto (type I) distribution are $G(x;\psi) = 1-\left(\frac{\alpha}{x}\right)^\gamma$ and $g(x;\psi) = \frac{\gamma\alpha^\gamma}{x^{\gamma+1}}$ respectively, where $\gamma > 0$ and $x \geq \alpha$. Setting the Pareto (type I) distribution as the baseline, we have the type I heavy-tailed odd Burr III-Pareto (TI-HT-OBIII-P) distribution with cdf

$$F(x;\theta,\gamma,\alpha,c,k) = 1-\left(\frac{1-[1+B_3(x;a,c,\gamma)]^{-k}}{1-(1-\theta)[1+B_3(x;a,c,\gamma)]^{-k}}\right)^\theta$$

and the pdf is

$$f(x;\theta,\gamma,\alpha,c,k) = \frac{\theta^2 ck\frac{\gamma\alpha^\gamma}{x^{\gamma+1}}[1+B_3(x;a,c,\gamma)]^{-k-1}\left[\left(\frac{\alpha}{x}\right)^\gamma\right]^{c-1}}{\left[1-\left(\frac{\alpha}{x}\right)^\gamma\right]^{c+1}[1-(1-\theta)[1+B_3(x;a,c,\gamma)]^{-k}]^{(\theta+1)}} \times \{1-[1+B_3(x;a,c,\gamma)]^{-k}\}^{\theta-1}$$

respectively for $\theta,\gamma,\alpha,c,k>0$ and $B_3(x;a,c,\gamma) = \left(\frac{\alpha^\gamma}{x^\gamma-\alpha^\gamma}\right)^c$.

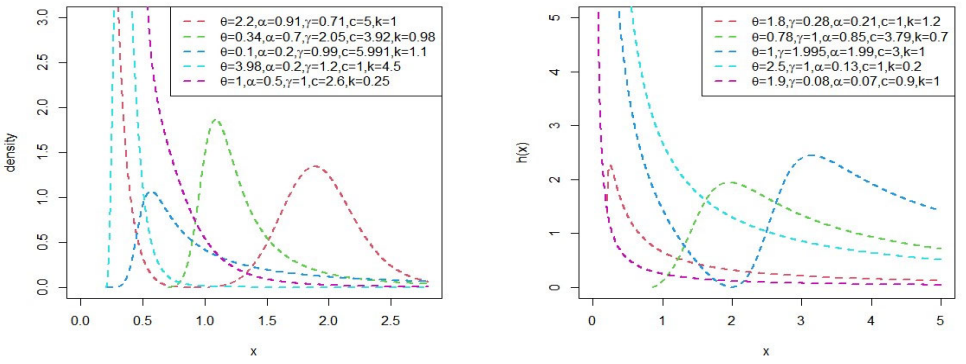

Figure 3: Pdf and hrf plots for the TI-HT-OBIII-P distribution

Density and hrf plots for the TI-HT-OBIII-P distribution are depicted in Figure 3. The TI-HT-OBIII-P density is capable of handling data that is positively-skewed, reversed-J and almost symmetric. The distribution's hrf displays inverted bathtub, decreasing and bathtub followed by inverted bathtub shapes.

3. Maximum Likelihood Estimation

The process of estimating unknown parameters for the TI-HT-OBIII-G FoD was carried out using the maximum likelihood estimation (MLE) technique. Consider a parameter vector $\Delta = (c, k, \theta, \Psi)^T$ and $X_i \sim$ TI-HT-OBIII-G. Using $\ell = \ell(\Delta)$ to denote the log-likelihood function, we have

$$\begin{aligned}\ell(\Delta) = {} & 2n\ln(\theta) + n\ln(c) + n\ln(k) + \sum_{i=1}^{n} \ln[g(x_i;\Psi)] \\ & -(k+1)\sum_{i=1}^{n} \ln\left[1+\left(\frac{1-G(x_i;\Psi)}{G(x_i;\Psi)}\right)^c\right] \\ & +(c-1)\sum_{i=1}^{n} \ln\big(1-G(x_i;\Psi)\big) - (c+1)\sum_{i=1}^{n} \ln\big(G(x_i;\Psi)\big) \\ & +(\theta-1)\sum_{i=1}^{n} \ln\left\{1-\left[1+\left(\frac{1-G(x_i;\Psi)}{G(x_i;\Psi)}\right)^c\right]^{-k}\right\} \\ & -(\theta+1)\ln\sum_{i=1}^{n}\left\{1-(1-\theta)\left[1+\left(\frac{1-G(x_i;\Psi)}{G(x_i;\Psi)}\right)^c\right]^{-k}\right\}.\end{aligned}$$

The MLEs of $(c, k, \theta$ and $\Psi_k)$ are obtained by solving a system of non-linear equations $\left(\frac{\partial \ell}{\partial c}, \frac{\partial \ell}{\partial k}, \frac{\partial \ell}{\partial \theta}, \frac{\partial \ell}{\partial \Psi_k}\right)^T = \mathbf{0}$ using iterative methods in R. See web **appendix** for individual components of the score vector.

4. Risk measures

Risk measures are statistical tools and formulae used by actuaries to evaluate market risk in prospective investments. These metrics encompass the value at risk (VaR), tail variance (TV), tail value at risk (TVaR), and tail variance premium (TVP).

4.1. VaR

VaR quantifies the magnitude of prospective financial losses over a specified time frame. VaR_q for the TI-HT-OBIII-G FoD is calculated from

$$X_q = G^{-1}\left(\left\{1+\left[\left(\frac{1-(1-u)^{\frac{1}{\theta}}}{1-(1-u)^{\frac{1}{\theta}}[1-\theta]}\right)^{\frac{-1}{k}}-1\right]^{\frac{1}{c}}\right\}\right)^{-1}, \tag{10}$$

where $q \in (0,1)$ specifies the significance level.

4.2. TVaR

TVaR computes expected loss value, considering the occurrence of an event exceeding a predefined probability threshold. TVaR for the TI-HTOBIII-G FoD is

$$\begin{aligned} TVaR_q &= E\left(X \mid X > x_q\right) = \frac{1}{1-q}\int_{VaR_q} xf(x)dx \\ &= \frac{1}{1-q}\sum_{w=0}^{\infty} \eta_{w+1}\int_{VaR_q}^{\infty} xg_{w+1}(x;\Psi)dx \end{aligned} \tag{11}$$

where η_{w+1} is provided by Equation (9), $g_{w+1}(x;\Psi)$ represents the Expon-G pdf and $(w+1)$ is the power parameter.

4.3. TV

TV captures the extent of variability in losses given that they exceed a predefined VaR threshold with a specific probability, denoted as p. The TV of the TI-HT-OBIII-G FoD is

$$\begin{aligned} TV_q &= E\left(X^2 \mid X > x_q\right) - \left(TVaR_q\right)^2 \\ &= (1-q)^{-1}\int_{VaR_q}^{\infty} x^2 f(x)dx - \left(TVaR_q\right)^2 \\ &= (1-q)^{-1}\sum_{w=0}^{\infty} \eta_{w+1}\int_{VaR_q}^{\infty} x^2 g_{w+1}(x;\Psi)dx - \left(TVaR_q\right)^2, \end{aligned} \tag{12}$$

where η_{w+1} is defined by Equation (9) and $g_{w+1}(x;\Psi)$ defines the Expon-G distribution. Hence, the TV of TI-HT-OBIII-G FoD can be derived from those of Expon-G distributions.

4.4. TVP

Risk professionals are fretful about risks exceeding certain thresholds. Such situations are common in insurance, for example, in policies involving deductibles and reinsurance contracts. Tail value premium answers demands to these circumstances. The TVP of the TI-HT-OBIII-G FoD is expressed as

$$TVP_q = TVaR_q + \delta(TV_q), \tag{13}$$

for $0 < \delta < 1$. The TI-HT-OBIII-G FoD TVP is found by incorporating Equations (11) and (12) into Equation (13).

4.5. Numerical analysis of risk measures

We provide findings from numerical simulations for the risk measures associated with the TI-HT-OBIII-W distribution. These risk measures were then compared among various distributions, including the type-I heavy-tailed Weibull (TI-HT-W), the two-parameter Weibull, and the one-parameter Weibull distributions. The simulation results were derived by implementing the following procedure:

(1) for each of the distributions under consideration, 100 random samples were generated, and the MLE method was used to estimate the parameters.

(2) 1000 replications were made in computing the risk measures these distributions.

Table 1: Numerical simulation results for risk measures

Distribution	Risk measure	0.70	0.75	0.80	0.85	0.90	0.95	0.99
TI-HT-OBIII-W ($\theta = 0.77, \lambda = 1.3, c = 1.4, k = 0.5$)	VaR	20.4389	22.5339	24.9911	28.0229	32.0982	38.6792	52.7591
	TVaR	29.4737	31.3723	33.6538	36.5297	40.4637	46.8901	48.7331
	TV	128.0030	130.5836	132.0992	134.9406	136.9434	293.2358	317.0861
	TVP	117.6757	124.0600	129.7331	134.2292	136.7127	135.4641	371.6070
TI-HT-W ($\theta = 0.77, \lambda = 1.3, \gamma = 0.04$)	VaR	18.4988	20.4513	22.7442	25.5754	29.3817	35.5251	48.6520
	TVaR	27.3904	29.1343	31.2249	33.8559	37.4539	39.0051	41.024
	TV	94.5879	99.0216	105.7756	112.1283	115.8558	124.8394	207.4612
	TVP	94.3019	99.2408	103.8454	107.9151	111.0971	185.2480	316.6550
Weibull ($\lambda = 1.3, \gamma = 0.04$)	VaR	13.6867	15.2406	17.0794	19.3654	22.4561	27.4667	38.1923
	TVaR	4.2572	5.1467	5.5777	5.9509	6.4436	6.4884	6.6304
	TV	79.8871	86.1114	102.2430	107.9056	110.8282	160.7040	166.8418
	TVP	66.0646	74.7844	81.3720	89.8165	93.7026	101.9418	112.4681
Weibull ($\lambda = 1.3$)	VaR	0.0701	0.0790	0.0896	0.1029	0.1212	0.1514	02182
	TVaR	0.0945	0.1021	0.1345	0.2310	0.2410	0.2610	0.3102
	TV	0.0213	0.0246	0.0294	0.0362	0.0483	0.0777	0.2197
	TVP	0.0149	0.0184	0.0234	0.0307	0.0435	0.0738	0.2175

Table [1] shows the findings of the risk metrics for the three heavy-tailed distributions. The model exhibiting elevated values of the risk measures implies that the model has a more pronounced tail. We can infer from the comparison that the TI-HT-OBIII-W distribution exhibits a heavier tail compared to both the TI-HT-W distribution and the Weibull distributions. As a result, the TI-HT-OBIII-W distribution is considered appropriate for modeling data sets with heavy-tail characteristics.

5 Simulation Study

We seek to weigh the efficiency of MLEs by carrying out a simulation study. Table 2 gives simulation results. We simulated for n= 35, 70, 140, 280, 560, 1120 and 2240 for N=3000 from the TI-HT-OBIII-W distribution. Average bias (AvBIAS) and root mean square error (RMSErr) for an estimated parameter, say (β), are computed as follows:

$AvBIAS(\hat{\beta}) = \frac{\sum_{i=1}^{N} \hat{\beta}_i}{N} - \beta,$ and $RMSErr(\hat{\beta}) = \sqrt{\frac{\sum_{i=1}^{N} (\hat{\beta}_i - \beta)^2}{N}}$, respectively.

Regarding the displayed data in Tables 2, it is evident that the average estimated parameter values converge towards the true parameter values. Additionally, both the RMSErr and AvBIAS decrease towards zero across all parameters as we increase the sample size. This shows that the TIHT-OBIII-W distribution produces consistent and efficient parameter estimates.

Table 2: Monte Carlo Simulation Results

Parameter	n	(0.8, 1.1, 1.1, 0.6)			(0.9, 1.0, 0.8, 1.2)		
		Mean	RMSErr	AvBias	Mean	RMSErr	AvBias
θ	35	1.4503	1.6864	0.6503	1.4685	1.1435	0.5685
	70	1.2697	1.0268	0.4697	1.3473	1.0018	0.4473
	140	1.0496	0.6277	0.2496	1.2106	0.9649	0.3106
	280	0.9591	0.4094	0.1591	1.1390	0.7247	0.2390
	560	0.8828	0.2049	0.0828	1.0796	0.4049	0.1796
	1120	0.8551	0.1012	0.0551	0.9789	0.1716	0.0789
	2240	0.8310	0.0714	0.0310	0.9176	0.0380	0.0176
λ	35	2.0024	2.2259	1.4024	1.1118	0.2362	0.2118
	70	1.9122	1.6588	0.9122	1.0757	0.1140	0.1757
	140	1.7680	1.5527	0.6680	1.0566	0.0965	0.1466
	280	1.6235	1.1358	0.5235	1.0419	0.0604	0.1219
	560	1.5244	0.9048	0.4244	1.0285	0.0372	0.1085
	1120	1.3954	0.6954	0.2954	1.0227	0.0166	0.0927
	2240	1.2982	0.4760	0.1982	1.0205	0.0078	0.0605

Table 2: Monte Carlo Simulation Results

Parameter	n	(0.8, 1.1, 1.1, 0.6)			(0.9, 1.0, 0.8, 1.2)		
		Mean	RMSErr	AvBias	Mean	RMSErr	AvBias
c	35	1.3164	1.5108	0.2164	1.0165	0.8932	0.2069
	70	1.2170	0.4721	0.1170	0.9508	0.5928	0.2052
	140	1.2118	0.3613	0.1118	0.9332	0.4495	0.2027
	280	1.2012	0.2484	0.1012	0.9235	0.3788	0.1765
	560	1.1893	0.2168	0.0893	0.8573	0.3268	0.1668
	1120	1.1691	0.1764	0.0691	0.8348	0.2596	0.1492
	2240	1.1434	0.1180	0.0634	0.8131	0.2013	0.0835
k	35	1.5605	2.6207	0.9605	2.1491	3.2232	0.9491
	70	1.2535	1.2710	0.6535	1.9198	1.6246	0.7198
	140	0.9593	0.8515	0.3593	1.7307	1.2020	0.5307
	280	0.8355	0.5619	0.2355	1.6073	1.0181	0.4073
	560	0.7250	0.2926	0.1250	1.5180	0.6697	0.3180
	1120	0.6515	0.1475	0.0815	1.3500	0.4386	0.1500
	2240	0.6437	0.1162	0.0737	1.2286	0.2114	0.0486

6. The TI-HT-OBIII-W regression model

The process of conducting a regression analysis on lifetime data entails determining the distribution of a variable X based on a set of covariates $\mathbf{u} = (\mathbf{u}_1, \ldots, \mathbf{u}_z)^T$. Within this context, we present a regression model for the TIHT-OBIII-W distribution which is designed to handle both censored and uncensored data. By letting c=1, we establish a relationship between the parameter λ and the covariates using a log-linear link function $\lambda_j = \exp(\mathbf{u}^T{}_j \beta)$ for $j = 1, \ldots, n$ and $\beta = (\beta_1, \beta_2, \beta_z)^T$ represents a vector comprising the regression coefficients. The survival function of $X \mid u$ is

$$S(X \mid u) = \left(\frac{1-\left[1+\left(\frac{\exp\left(-x^{\exp\left(u^T\beta\right)}\right)}{1-\exp\left(-x^{\exp\left(u^T\beta\right)}\right)}\right)\right]^{-k}}{1-(1-\theta)\left[1+\left(\frac{\exp\left(-x^{\exp\left(u^T\beta\right)}\right)}{1-\exp\left(-x^{\exp\left(u^T\beta\right)}\right)}\right)\right]^{-k}} \right)^{\theta}. \tag{14}$$

The parametric regression model, known as the TI-HT-OBIII-W, is denoted by Equation (14). If we consider A and S as two separate groups of individuals, where x_j represents the lifetime of individuals in set A and S represents the censoring information, the overall log-likelihood function for the parameter vector $\Delta = (\theta, \beta^T, k)^T$ derived from Equation (14) can be expressed in the form $\ell(\Delta) = \sum_{j \in A} \ell_j(\Delta) + \sum_{j \in S} \ell_j^s(\Delta)$,

where $\ell_j(\Delta) = \log(f(x_j \mid u_j))$, $\ell^s_j(\Delta) = \log(S(x_j \mid u_j))$ and $f(x_j \mid u_j)$, $S(x_j \mid u_j)$ represent the density and survival functions of X, respectively. Let ρ take the value 0 if censoring occurs and 1 if failure is observed. Then the expression for the log-likelihood function for Δ can be expressed as

$$\begin{aligned}
\ell(\Delta) = {} & 2n\rho \ln(\theta) + n\ln(k) + \sum_{j\in A}^{n} \ln\left[\exp\left(u_j^T\beta\right) x_j^{\exp\left(u_j^T\beta\right)-1} \exp\left(-x_j^{\exp\left(u_j^T\beta\right)}\right)\right] \\
& - (k+1)\sum_{j\in A}^{n} \ln\left[1 + \left(\frac{\exp\left(-x_j^{\exp\left(u_j^T\beta\right)}\right)}{1-\exp\left(-x_j^{\exp\left(u_j^T\beta\right)}\right)}\right)\right] + 2\sum_{j\in A}^{n} \ln\left(1 - \exp\left(-x_j^{\exp\left(u_j^T\beta\right)}\right)\right) \\
& + (\theta-1)\sum_{j\in A}^{n} \ln\left\{1 - \left[1 + \left(\frac{\exp\left(-x_j^{\exp\left(u_j^T\beta\right)}\right)}{1-\exp\left(-x_j^{\exp\left(u_j^T\beta\right)}\right)}\right)\right]^{-k}\right\} \\
& - (\theta+1)\ln\sum_{j\in A}^{n} \left\{1 - (1-\theta)\left[1 + \left(\frac{\exp\left(-x_j^{\exp\left(u_j^T\beta\right)}\right)}{1-\exp\left(-x_j^{\exp\left(u_j^T\beta\right)}\right)}\right)\right]^{-k}\right\} \\
& + \theta\sum_{j\in S} \log(1-\rho)\left[\left(\frac{1 - \left[1 + \left(\frac{\exp\left(-x_j^{\exp\left(u_j^T\beta\right)}\right)}{1-\exp\left(-x_j^{\exp\left(u_j^T\beta\right)}\right)}\right)\right]^{-k}}{1-(1-\theta)\left[1 + \left(\frac{\exp\left(-x_j^{\exp\left(u_j^T\beta\right)}\right)}{1-\exp\left(-x_j^{\exp\left(u_j^T\beta\right)}\right)}\right)\right]^{-k}}\right).
\end{aligned} \tag{15}$$

The MLE $\hat{\Delta}$ of the vector of unknown parameters can be obtained by maximizing Equation (15) using R software. We also consider residuals for the TI-HT-OBIII-W regression model. By plotting the deviance residuals against the index (numerical identifier assigned to each observation in the dataset), one can effectively identify and validate the appropriateness of the fitted model for a typical observation. The deviance residual, which serves as a measure of the disparity between the observed values and the predicted values, can be mathematically defined as

$$r_{Di} = sign(r_{Mi})\,(-2[r_{Mi} + \rho_i \log(\rho_i) - r_{Mi}])^{0.5},$$

where r_{Mi} is the martingale residual defined by

$$r_{M_i} = \begin{cases} 1 + log\left[\left(\dfrac{1-\left[1+\left(\dfrac{exp\left(-x_j^{\,exp\left(u_j{}^T\beta\right)}\right)}{1-exp\left(-x_j^{\,exp\left(u_j{}^T\beta\right)}\right)}\right)\right]^{-k}}{1-(1-\theta)\left[1+\left(\dfrac{exp\left(-x_j^{\,exp\left(u_j{}^T\beta\right)}\right)}{1-exp\left(-x_j^{\,exp\left(u_j{}^T\beta\right)}\right)}\right)\right]^{-k}}\right)^{\theta}\right] & if\ \rho_{i=1}, \\ log\left[\left(\dfrac{1-\left[1+\left(\dfrac{exp\left(-x_j^{\,exp\left(u_j{}^T\beta\right)}\right)}{1-exp\left(-x_j^{\,exp\left(u_j{}^T\beta\right)}\right)}\right)\right]^{-k}}{1-(1-\theta)\left[1+\left(\dfrac{exp\left(-x_j^{\,exp\left(u_j{}^T\beta\right)}\right)}{1-exp\left(-x_j^{\,exp\left(u_j{}^T\beta\right)}\right)}\right)\right]^{-k}}\right)^{\theta}\right] & if\ \rho_{i=0}. \end{cases}$$

and sign (.) assigns the values of +1 when the argument is positive, and −1 when the argument is negative.

In the work by Atkinson (1985), a technique was proposed to create envelopes that facilitate the enhanced analysis of the normal probability plot of residuals. These envelopes, sometimes referred to as simulated confidence bands, are constructed to encompass the residuals. The anticipation is that when the model is suitably fitted, most data points will align within these specified ranges and demonstrate a random distribution.

7. Applications

Real data examples are fitted to the TI-HT-OBIII-W distribution and compared to several non-nested models including some known heavy-tailed distributions and equiparameter models. The TI-HT-OBIII-W distribution is compared to the transmuted exponentiated generalized Weibull distribution (TExGW) proposed by Yousof et al. (2015), the type I heavy-tailed Weibull distribution (TI-HT-W) introduced by Zhao et al. (2020), the heavy-tailed beta power transformed Weibull distribution (HTBPTW) introduced by Zhao et al. (2021), the Weibull Lomax distribution (WL) by Tahir et al. (2014), Kumaraswamy Weibull distribution (KW) introduced by Cordeiro et al. (2010) and the exponential Lindley odd log-logistic Weibull (ELOLLW) proposed by Korkmaz et al. (2018). Visit the web **appendix** for the pdfs of distributions used in the comparisons.

We presented the goodness-of-fit (Gof) statistics: -2 log-likelihood (-2log(L)), Akaike Information Criterion (AIC), Consistent Akaike Information Criterion (CAIC), Bayesian Information Criterion (BIC), Cramér-von Mises (W^*) and Andersen-Darling (A^*). These statistics are used to verify the best-fitting model for a given data set. Reduced values of these metrics indicate that the model is a better fit compared to other competing models.

Gof was also assessed by the Kolmogorov-Smirnov (K-S) statistic, its associated p-value, and the sum of squares (SS) derived from probability plots. The model that exhibits the smallest K-S value and the highest p-value for the K-S statistic is considered as the best-fitting model. Furthermore, graphical presentations of the fitted densities and probability-probability (PP) plots, empirical cumulative distribution function (ECDF), Kaplan-Meier (K-M) survival, total time on test (TTT) plots and hrf plots were presented.

7.1. Stress-rupture life data

The initial dataset showcases the stress-rupture life of Kevlar 49/epoxy strands under continuous sustained pressure at a 90% stress level until failure. This practical example was originally presented by Cooray and Ananda (2008), and subsequently reported by Cordeiro et al. (2014). The data can be found in the **appendix**.

The asymptotic confidence intervals at a 95% confidence level for the model parameters are as follows:
$\theta \in [0.7055 \pm 0.4243]$, $\lambda \in [0.9911 \pm 0.3556]$, $c \in 1.2942 \pm 0.9120]$ and $k \in [0.5288 \pm 0.60409]$.

The estimated variance-covariance matrix is

$$\begin{bmatrix} 0.0469 & 0.0030 & -0.0830 & 0.0647 \\ 0.0030 & 0.0329 & -0.0473 & 0.0009 \\ -0.0830 & -0.0473 & 0.2165 & -0.1141 \\ 0.0647 & 0.0009 & -0.1141 & 0.0950 \end{bmatrix}.$$

Table 3: Parameter estimates on stress-rupture life data

Model	Estimates			
TI-HT-OBIII-W	θ	λ	c	k
	0.7055	0.9911	1.2942	0.5288
	(0.2165)	(0.1814)	(0.4653)	(0.3082)
TExGW	λ	a	b	β
	0.0011	0.8113	0.7930	1.0604
	(2.7424)	(2.0878)	(0.6052)	(1.0756)
TI-HT-W	α	θ	γ	
	0.8435	0.6277	1.9662	- -
	(0.0959)	(0.2431)	(0.9963)	
HBPTW	α	γ	k	
	0.8840	1.1239	1.7284	--
	(0.0995)	(0.2008)	(0.6056)	
WL	α	b	α	β
	0.2506	0.7860	1.3581	0.3303
	(0.4173)	(0.1804)	(0.4580)	(0.6282)
KW	α	b	α	β
	0.7280	0.3323	2.4974	1.0514
	(0.2699)	(0.5544)	(4.3669)	(0.1639)
ELOLLW	β	λ	θ	γ
	6.7617	0.1641	7.0720	0.8374
	(0.3733)	(0.0853)	(0.2268)	(0.0144)

The MLEs together with their standard errors (SEs) (in parenthesis) for the models on stress-rupture life data are given in Table 3 and Gof statistics are presented in Table 4. The profile plots in Figure [4] clearly show that the TI-HT-OBIII-W parameters on stress-rupture life data are global maximums and are identifiable.

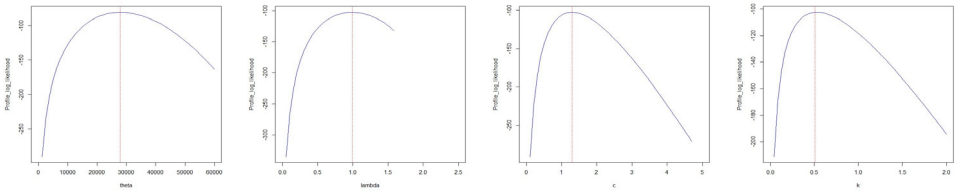

(a) (b) (c) (d)

Figure 4: Profile plots for the TI-HT-OBIII-W parameters: Stress-rupture life data

Table 4: Gof statistics on stress-rupture life data

Model	2log(L)	AIC	CAIC	BIC	W^*	A^*	K-S	p-value
TI-HT-OBIII-W	204.7661	212.7661	213.1827	223.2266	0.1255	0.7790	0.0679	0.7409
TExW	205.5743	213.5743	213.9910	224.0348	0.1652	0.9586	0.0844	0.4681
TI-HT-W	207.9245	213.9245	214.7905	219.9504	0.1703	0.9742	0.0786	0.5612
HBPTW	205.5669	211.5669	211.8144	219.4123	0.1864	1.0524	0.0854	0.4526
WL	205.1976	213.1976	213.6143	223.6581	0.1440	0.5627	0.0787	0.5587
KW	205.3001	213.3001	213.7183	223.7621	0.1414	0.1423	0.0773	0.5815
ELOLLW	205.1945	213.1945	213.6112	223.6550	0.1666	0.9601	0.0816	0.5126

Figure 4 shows profile plots for stress-rupture data. The plots illustrate that the TI-HT-OBIII-W parameters are global maximums and are identifiable. Figure 5 supports the dominance of TI-HT-OBIII-W model over the non-nested models on stress-rupture life data. Gof statistics and the p-values obtained on stress-rupture life data show that the TI-HT-OBIII-W model outperforms the various non-nested models that were evaluated.

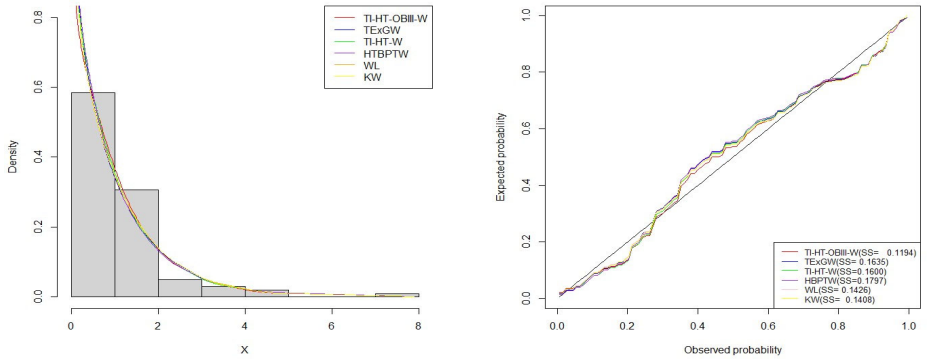

Figure 5: Graphical representations of fitted density functions and probability plots for stress-rupture life data

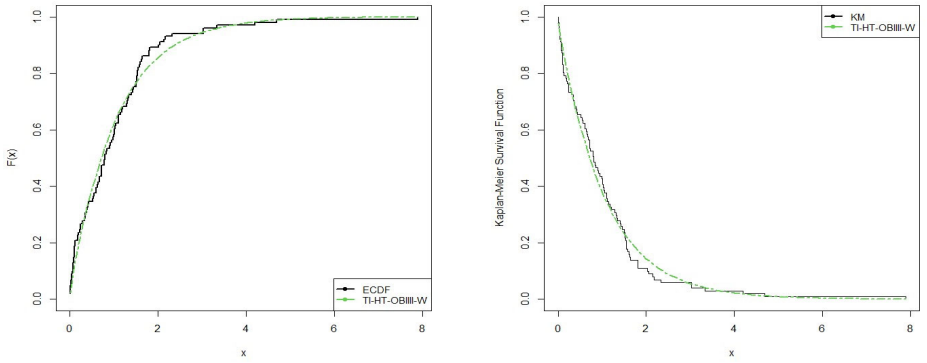

Figure 6: Fitted ECDF curve and K-M plots for stress-rupture life data

Figure 6 presents fitted and observed ECDF and K-M survival curves for stress-rupture life data. The plots show that the TI-HT-OBIII-W distribution closely follows the ECDF and K-M survival curves. The TTT scaled and hrf plots in Figure 7 generally show a sequence of a bathtub followed by an inverted bathtub hazard rate shapes for the stress-rupture life data.

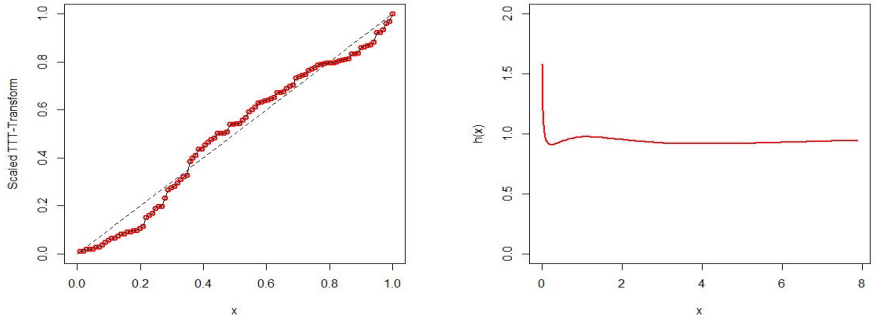

Figure 7: TTT scaled and hrf plots for stress-rupture life data

7.2. Turbocharger data

The second data set was taken from Xu et al. (2003), describing a reliability study on turbochargers in diesel engines. The data is presented in the **appendix**. The estimated MLEs accompanied by their corresponding SEs (in brackets), and GoF statistics for the turbochargers data are displayed in Table 5.

The asymptotic confidence intervals at a 95% confidence level for the model parameters are as follows: $\theta \in [\ 2.64\times10^{4}\pm\ 4.70\times10^{-4}]$, $\lambda \in [1.0278\pm0.6633]$,

$c \in [3.81\times10^{-2}\pm 6.90\times10^{-2}]$ and $k \in [36.3600 \pm 4.2571]$. The estimated variance-covariance matrix is

$$\begin{bmatrix} 5.76\times10^{-8} & 7.12\times10^{-5} & -7.83\times10^{-5} & 5.21\times10^{-4} \\ 7.12\times10^{-5} & 1.15\times10^{-1} & -1.18\times10^{-2} & -6.44\times10^{-1} \\ -7.83\times10^{-6} & -1.18\times10^{-2} & 1.24\times10^{-3} & 7.09\times10^{-2} \\ 5.21\times10^{-4} & -6.44\times10^{-1} & 7.09\times10^{-2} & 4.7200 \end{bmatrix}.$$

Table 5: Estimates on turbochargers data

Model	Estimates			
TI-HT-OBIII-W	θ	λ	c	k
	2.64×10^{4}	1.0278	5.76×10^{-8}	36.3600
	(2.40×10^{-4})	(0.3384)	(3.52×10^{-2})	(2.1720)
TExGW	λ	a	b	β
	0.0321	6.90×10^{-5}	0.6720	4.7712
	(5.21×10^{-10})	(1.31×10^{-5})	(9.07×10^{-10})	(1.85×10^{-9})
TI-HT-W	α	θ	γ	
	3.5513	0.6514	0.0019	- -
	(0.6241)	(0.3243)	(0.0033)	
HBPTW	α	γ	k	
	3.2828	0.0026	0.1490	- -
	(0.7116)	(0.0042)	(0.1766)	
WL	α	b	α	β
	0.7306	2.8721	2.12×10^{4}	1.98×10^{5}
	(0.1329)	(0.3790)	(1.69×10^{-5})	(1.82×10^{-6})
KW	α	b	α	β
	0.5021	89.1240	$4.51\times10^{4-2}$	7.6849
	(6.68×10^{-2})	$(2.65\times10^{4-6})$	$(6.72\times10^{4-3})$	$(4.36\times10^{4-3})$
ELOLLW	β	λ	θ	γ
	1.944	0.1393	1.7917	3.4997
	(1.0760)	(0.0351)	(1.1969)	(0.6303)

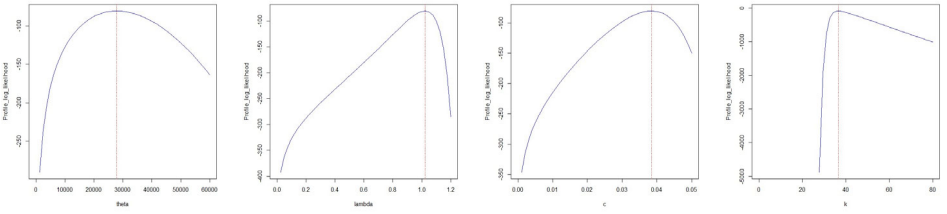

(a) (b) (c) (d)

Figure 8: Profile plots for the TI-HT-OBIII-W parameters: Turbochargers data

The Gof statistics and the K-S p-values obtained on reliability of turbochargers in diesel engines data also show that the TI-HT-OBIII-W model is superior to the several non-nested models that were considered. Figure 8 shows profile plots for turbochargers data. The plots illustrate that the TI-HT-OBIII-W parameters are global

maximums and are identifiable. Figure 9 shows that the TI-HT-OBIII-W model outperforms the non-nested models that were considered.

Table 6: Gof statistics on turbochargers life data

Model	2log(L)	AIC	CAIC	BIC	W^*	A^*	K-S	p-value
TI-HT-OBIII-W	160.4252	168.4252	169.5681	175.1808	0.0350	0.2581	0.0752	0.9775
TExW	160.7456	168.7456	171.8885	177.5011	0.0579	0.4441	0.1069	0.7511
TI-HT-W	164.2436	170.2436	170.9103	175.3102	0.0674	0.5073	0.1005	0.8143
HBPTW	163.5073	169.5073	170.1740	174.5739	0.0592	0.4493	0.0977	0.8396
WL	162.3950	170.3950	171.5379	177.1505	0.0522	0.4018	0.1001	0.8173
KW	164.7952	172.7952	173.9381	179.5507	0.0755	0.5633	0.1076	0.7430
ELOLLW	163.7752	171.7752	172.9181	178.5308	0.0636	0.4815	0.1017	0.8028

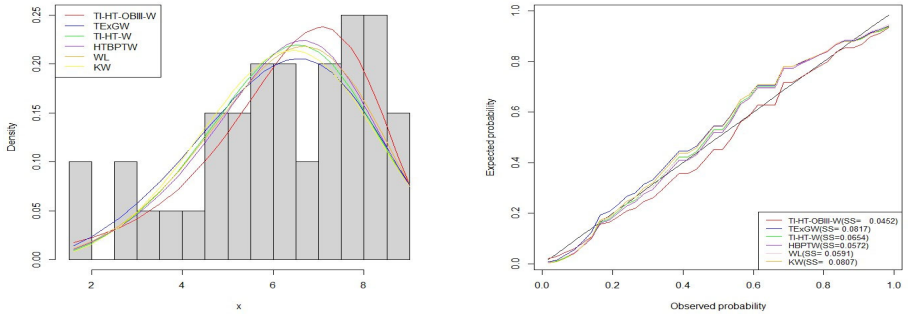

Figure 9: Visualizations of fitted density functions and probability plots for turbochargers data.

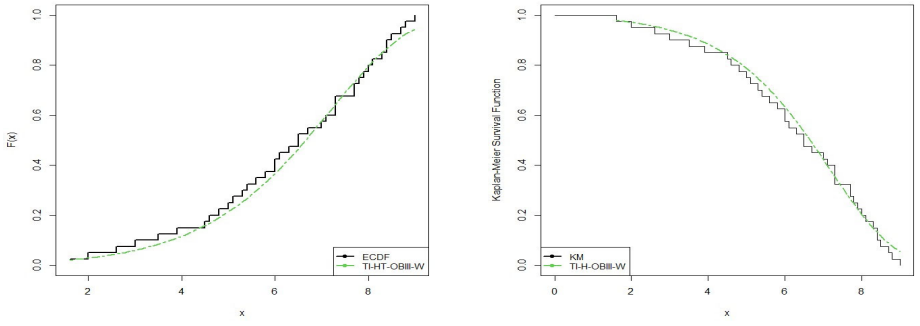

Figure 10: Fitted ECDF curve and K-M plots for turbochargers data

Figure 10 exhibits the convergence between the empirical and the fitted ECDF and K-M survival curves, for turbocharger data. We can see that the TI-HT-OBIII-W demonstrates a remarkable alignment with both the ECDF and K-M survival curves, indicating a close correspondence between the observed and fitted data. The TTT scaled

plot and hrf plots depicted in Figure 11 provide clear evidence that the data shows an increasing hazard rate.

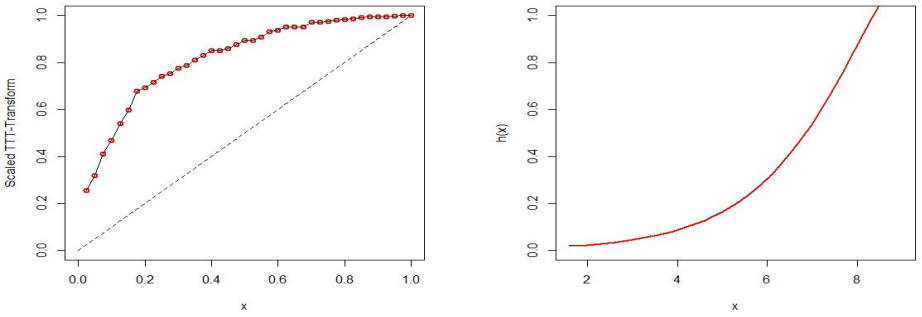

Figure 11: TTT scaled and hrf plots for turbochargers data

7.3. Regression model for transformer turns data

This real data set is sourced from Nelson (2004) and represents a life testing of transformers conducted at high voltage, resulting in multiple censored data. The failures observed in the study were turn-to-turn failures of the primary insulation with 13% censored observations. The data includes observations at three different voltage levels (35.4kV, 42.4kV, and 46.7kV), and the symbol $(*)$ indicates instances of censored data. The data set can be found in the **appendix** section. Firstly, we examine the TI-HT-OBIII-W, TI-HT-W and ELOLLW distributions for the transformer turns data presented in Table 8. MLEs and their SEs (in parentheses) are provided for these distributions. Additionally, we report the -2log(L), AIC, and BIC Gof statistics associated with the fitted models.

The variables considered in this study are x_j=time of failure in hours of the transformer, j = 1, 2, ...,30, and three voltage levels defined by (35.4kV, 42.4kV and 35.4kV).

Table 7: Estimates and Gof statistics transformer turns data

Distribution	Parameter estimates			
TI-HT-OBIII-W	θ	λ	c	k
	2.3871	0.2362	0.9342	11.6409
	0.1361	0.0307	0.3875	0.2855
ELOLLW	β	λ	θ	γ
	0.0011	0.0241	0.7767	0.7185
	(0.2866)	(0.0144)	(6.24×10^{-4})	(0.1034)
TI-HT-W	α	θ	γ	k
	0.7105	1.17×10^{-3}	47.4190	11.6409
	(0.1024)	(6.12×10^{-4})	(1.93×10^{-6})	0.2855

Table 8: Gof statistics on transformer turns data.

Distribution	Gof Statistics				
	−2log(L)	AIC	CAIC	BIC	*SS*
TI-HT-OBIII-W	267.4544	212.7661	213.1827	223.2266	0.0455
ELOLLW	270.6383	213.5743	213.991	224.0348	0.1052
TI-HT-W	270.2332	211.5669	211.8144	219.4123	0.0623

We consider the following structured regression

$$\lambda_j = \exp(\beta_{10} + \beta_{11}u_{j1} + \beta_{12}u_{j2}),$$

where u_{j1} and u_{j2} are the covariates representing the predictor variables for j = 1,2,3, ...,30, to maximize the log-likelihood function in Equation (17) to obtain the MLEs of the parameters of the proposed model. We provide the parameter estimates, SEs, and the significance of the MLEs in Table 9. The findings presented in Table 9 offer convincing empirical support, at a significance level of 5%, indicating a substantial disparity between the 35kV level and the 46.7 kV level.

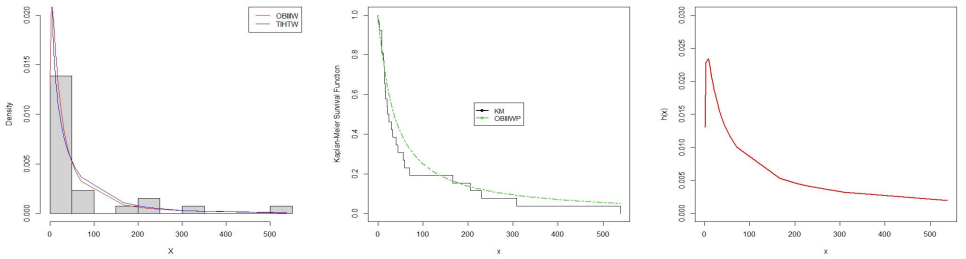

Figure 12: Fitted models: Histogram, K-M curve and hrf plot for transformer turns data

Figure 12 displays the histograms and fitted densities of the TI-HT-OBIII-W and TI-HT-W distributions. The K-M survival curve demonstrates that the TIHT-OBIII-W closely corresponds to the transformer turns data. The hrf curve indicates an inverted hazard rate shape.

Table 9: MLEs for regression model fitted to transformer turns

Parameters	Estimate	SE	p-value
θ	0.5000	0.1515	--
k	3.7576	7.33×10^{-4}	--
β_{10}	7.43×10^{-4}	0.0104	0.3109
β_{11}	0.0659	0.0162	<0.00001
β_{12}	-0.0269	0.2687	0.0978

7.4. Goodness-of-fit

We present the results of the residual analysis in Figure 13, specifically focusing on the deviance component residual r_{Di} discussed in Section 6. In the deviance residual vs index plot, we observe a prominent outlier, indicating a significant deviation from the expected pattern. However, when considering the normal probability plot along with the generated envelope, we find that approximately 93% of the data points fall within the envelope. This suggests that the proposed TI-HT-OBIII-W regression model is indeed appropriate for these data, as only a single observation lies outside the expected range.

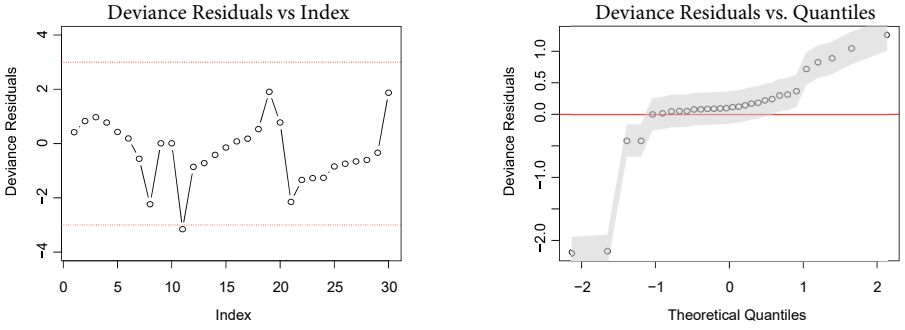

Figure 13: Plot of deviance residuals against index and normal probability plot with envelopes for the deviance component residuals.

8. Summary

We developed and presented a new heavy-tailed FoD called the type I heavy-tailed odd Burr III-G (TI-HT-OBIII-G) distribution. Statistical properties of this new FoD were derived and presented. The MLE technique was utilized in the estimation of parameters. Actuarial risk measures were computed. Numerical comparisons of actuarial measures with other distributions were conducted and the results were presented. The regression model and the analysis of residuals were examined in the context of the new distribution. Finally, the superiority of the TI-HT-OBIII-G FoD was illustrated by the Kevlar 49/epoxy strands and turbocharger data sets. We recommend bivariate regression models and different parameter estimation techniques for future research.

***To access the appendix, kindly click the link provided below*:**
https://drive.google.com/file/d/1KEtYcoHXU3FhE4OK8DvdFSg5v01_Qi1M/view?usp=sharing

References

Afify, A. Z., Gemeay, A. M. and Ibrahim, N. A., (2020). The Heavy-Tailed Exponential Distribution: Risk Measures, Estimation, and Application to Actuarial Data. *Mathematics*, 8(8), 1276.

Alizadeh, M., Cordeiro, G., Nascimento, A. and M. Ortega, E. M. M. (2017). Odd Burr Generalized Family of Distributions with some Applications. *Journal of Statistical Computation and Simulation*, 87, pp. 367–389.

Alyami, S. A., Babu, M. G., Elbatal, I., Alotaibi, N. and Elgarhy, M., (2022). Type II Half Logistical Odd Fréchet Class of Distributions: Statistical Theory and Applications. *Symmetry*, 14(6), 1222. https://doi.org/10.3390/sym14061222

Atiknson, A. C., (1985). Plots, Transformations and Regression: An Introduction to Graphical Methods of Diagnostic Regression Analysis. *Clarendon Press Oxford*. https://doi.org/10.1007/s40300-013-0007

Benkhelifa, L., (2022). Alpha Power Topp-Leone Weibull Distribution: Properties, Characterizations, Regression Modeling and Applications. *Journal of Statistics and Management Systems*, 25(8), pp. 1–26.

Cooray, K., Ananda, M. M., (2008). A Generalization of the Half-normal Distribution with Applications to Lifetime Data. *Communications in Statistics Theory and Methods*, 37(9), pp. 1323–1337.

Cordeiro, G. M., Alizadeh, M. and Ortega, E. M., (2014). The Exponentiated Half-Logistic Family of Distributions: Properties and Applications. *Journal of Probability and Statistics*. https://doi.org/10.1155/2014/864396

Cordeiro, G. M., Ortega, E. M. and Nadarajah, S., (2010). The Kumaraswamy Weibull Distribution with Application to Failure Data. *Journal of the Franklin Institute*, 347(8), pp.1399–1429.

Dey, S., Nassar. M. and Kumar, D., (2019). Alpha Power Transformed Inverse Lindley Distribution. A Distribution with an Upside-down Bathtub shaped Hazard Function. *Journal of Computational and Applied Mathematics*, 348, pp. 130-145.

Descheemaeker, L., Grilli. J. and de Buyl, S., (2021). Heavy-tailed Abundance Distributions from Stochastic Lotka-Volterra models. *American Physical Society*, 104(38), pp. 034404-034413.

Korkmaz, M. C., Yousof, H. M. and Hamedani, G. G., (2018). The Exponential Lindley odd Log-Logistic-G Family: Properties, Characterizations and Applications. *Journal of Statistical Theory and Applications*, 17(3), pp. 554–571.

Nelson, W. B., (2004). Accelerated Testing: Statistical Models, Test Plans, and Data Analysis. *John Wiley and sons*.

Rényi, A., (1960). On Measures of Entropy and Information. Proceedings of the Fourth Berkeley. *Symposium on Mathematical Statistics and Probability*.

Shannon, C. E., (1951). Prediction and Entropy of Printed English. *The Bell System Technical Journal*.

Tahir, M., Cordeiro, G. M. and Zubair, M., (2014). The Weibull-Lomax distribution: Properties and Applications. *Hacettepe University Bulletin of Natural Sciences and Engineering Series B: Mathematics and Statistics*, 10, pp. 147-465.

Teamah, A. E. A., Elbanna, A. A. and Gemeay, A. M., (2021). Heavy-tailed Log-Logistic Distribution: Properties, Risk Measures and Applications. *Statistics, Optimization, and Information Computing*, 9(4), pp. 910-941.

Xu, K., Xie, M., Tang, Ching, L. and Ho, S. L., (2003). Application of Neural Networks in Forecasting Engine Systems Reliability. *Applied Soft Computing*, 2, pp. 255-268.

Yousof, H. M., Afify, A. Z., Alizadeh, M., Butt, N. S., Hamedani, G. and Ali, M. M., (2015). The Transmuted Exponentiated Generalized-G Family of Distributions. *Pakistan Journal of Statistics and Operation Research*, 11(4), pp. 441-464.

Zhao, W., Khosa, S. K., Ahmad, Z., Aslam M., and Afify, A. Z., (2020). Type-I Heavy-Tailed Family with Applications in Medicine, Engineering, and Insurance. *PLoS ONE*, 15(8). https://doi.org/10.1371/journal.pone.0237462.